Calibration of a Model to Predict the Peak Punch-Through Penetration Resistance of a Spudcan on Sand Overlying Clay

S. A. Stanier, P. Hu and M. J. Cassidy
Centre for Offshore Foundation Systems, University of Western Australia

Abstract: This paper demonstrates the use of a geotechnical drum centrifuge in the calibration of a model to predict the peak punch-through penetration (q_{peak}) resistance of a spudcan on sand overlying clay. A series of loose sand overlying clay tests was performed and combined with an existing database of tests performed on dense sand overlying clay. The performance of the failure stress dependent model proposed by Lee (2009) and Lee et al. (2009) has then been assessed using this combined dataset which encompasses a wider range of soil properties and problem geometries than was used in the original calibration of the model. The single empirical stress distribution factor (D_F) that is employed in the model was then optimised using a back calculation procedure for all tests. The scatter of the optimised D_F values was then compared for the original bi-linear calibration proposed by Lee et al. (2009) and a new non-linear power law calibration. The new non-linear relationship enables the model to better predict q_{peak} over a wider range of problem geometries and for conditions of both loose and dense sands overlying clay. The work demonstrates the importance of the geotechnical centrifuge in calibrating such models given that at present numerical methods are unable to reliably capture such punch-through behaviour and good quality field data of punch-through failure of spudcan foundations is unavailable.

Keywords: Spudcan, punch-through, calibration, centrifuge, sand, clay.

1 INTRODUCTION

Modern jack-up structures typically consist of a triangular platform, through which three trussed legs, which are terminated with spudcan foundations, are jacked down onto the seabed. Ballast tanks on the platform are then filled with water to preload the spudcan foundations to a bearing pressure, q_{nom}, which is greater than the anticipated working loads. In a single deep layer of Normally Consolidated (NC) clay this is relatively straightforward since the undrained shear strength of the clay tends to increase with depth due to the effective stress profile. Thus during preloading the displacement of the foundations is usually relatively slow and controllable as bearing pressures increase with depth, as illustrated in Figure 1 (a). However, in sand overlying clay strata there is a danger that penetrating a relatively thin but stiff sand layer overlying a weak clay bed may lead to a peak in the measured penetration resistance, q_{peak}. If this peak penetration resistance is followed by a reduction in bearing pressure (caused by the underlying weaker clay soil), punch-through failure of one or more leg may occur. This is illustrated schematically in Figure 1 (b) and (c). This can lead to buckling of the leg or in the worst cases even toppling of the platform. Baglioni et al. (1982) reported a rapid punch-through failure of a jack-up leg with penetration of 10 m in 30 seconds. The average cost to the operator of a jack-up rig of a punch-through incident was estimated by Osborne and Paisley (2002) to be in the range of US$1-10 million and numerous incidents still occur on an annual basis.

Therefore predicting the peak punch-through penetration resistance of a spudcan penetrating sand overlying clay is of key importance to the offshore oil and gas industry, both in terms of safety and economics. Unlike many geotechnical situations where a conservative calculation approach is suitable, in this situation it is imperative that the peak penetration resistance is calculated accurately. An accurate

estimate of the peak penetration resistance allows appraisal of the risk of punch-through and potentially the displacement induced by the punch-through event.

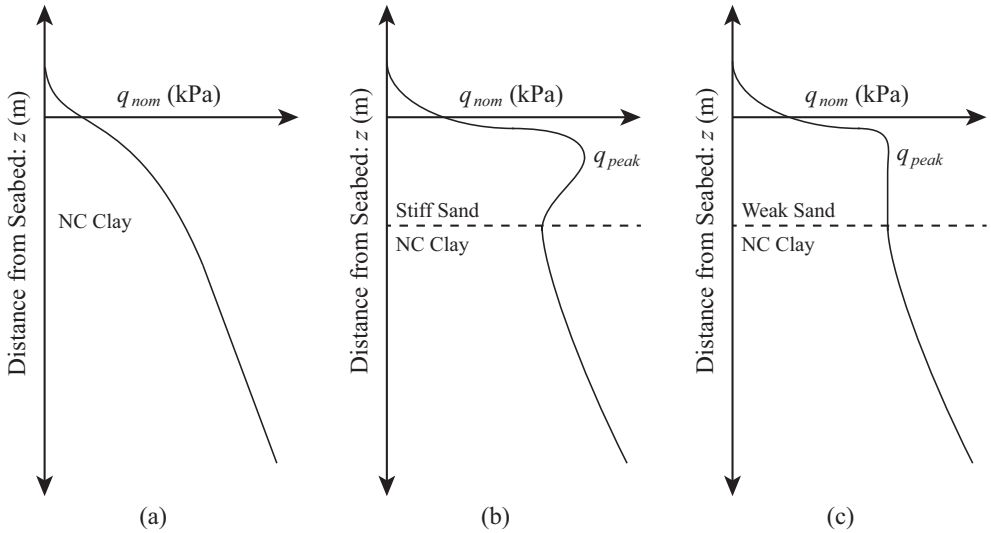

Figure 1: Penetration resistance profiles: safe installation on NC clay (a); serious punch-through failure on stiff sand overlying NC clay (b); and rapid run-out punch-through failure on weak sand overlying NC clay (c). Penetration distance plotted with reference to maximal diameter of the spudcan.

2 OVERVIEW OF PREDICTION METHODS

2.1 Current Best Practice

Current best practice for predicting peak punch-through resistance is outlined in SNAME (2002) and favours the mechanism of Hanna and Meyerhof (1980) for a foundation on sand overlying clay strata. The mechanism consists of a cylinder of sand punching through the underlying clay. The peak penetration resistance, q_{peak}, is determined by relating the normalised shear strength of the underlying clay to the product of the punching shear coefficient, K_s, and $\tan\phi'$:

$$K_s \tan\phi' = \frac{3s_u}{\gamma'_s D} \tag{1}$$

where s_u is the undrained shear strength of the clay, γ'_s is the effective unit weight of the sand layer and D is the foundation diameter. Recent observation of the failure mechanism within a geotechnical centrifuge by Teh et al. (2008) has shown this assumed failure mechanism to be inappropriate as in reality it consists of a truncated inverted cone of sand penetrating the underlying clay. An alternative failure mechanism based on the projected area method is suggested in the SNAME (2002) 'commentaries'. This mechanism is more consistent with the observations of Teh et al. (2008) as it assumes that the bearing pressures spread out through the sand layer allowing the bearing capacity to be estimated to be equal to that of an imaginary foundation of increased area at the depth of the sand-clay interface. There is no consensus on a suitable inclination angle α for this mechanism, consequently the SNAME (2002) 'commentaries' recommend a range of spreading ratios of 1h:3-5v based upon back calculations of field data.

However, neither of these approaches properly account for the sand properties in the upper sand layer, since even in the punching shear method the sand properties are expressed as a function of the shear strength of the underlying clay. In fact both methods have been demonstrated by Lee et al. (2009) to provide similar predictions of q_{peak}, as in both cases the relationship between q_{peak} and the bearing capacity of the underlying clay is simply a quadratic function of H_s/D.

2.2 Initial Stress Dependent Methods

Okamura et al. (1998) attempted to account for the properties of the sand layer and the impact of initial in-situ stress on its behaviour using Bolton's (1986) empirical relationships relating the dilatancy of sand to its stress state. The method combines the geometry of the projected area method whilst incorporating initial stress dependent dilatancy effects into the properties of the sand layer. However, Lee (2009) demonstrated that this method necessitates that larger ϕ' generates smaller angles of inclination in the failure mechanism. Given that sand with higher ϕ' is usually expected to be more dilatant, the angle of inclination would be more likely to increase with increasing ϕ'.

Similarly, Teh (2007) proposed a method accounting for the sand properties and initial stress state in the sand layer based upon Particle Image Velocimetry (PIV) visualisation experiments performed in the drum centrifuge. An inverted truncated cone shaped sand plug was seen to penetrate into the underlying clay, providing frictional resistance at its boundaries in the sand layer and bearing capacity in the clay at its base. The friction angle of the sand was taken as the average of the critical state friction angle, ϕ_{cv}, and the operative friction angle, which was related to the initial stress state following Okamura et al. (1998). The angle of inclination of the failure mechanism, α, was determined using semi-logarithmic design curves calibrated using five drum centrifuge tests of varying scale and geometry performed at UWA. Bearing capacity in the underlying clay was assumed to reduce with radial distance of the line of symmetry of the problem following semi-logarithmic design curves related to the H_s/D and q_{clay}/q_{sand} ratios. However, this method is geometrically inconsistent, since the bearing capacity in the sand layer is based upon a simple inverted truncated cone failure surface, whereas the bearing capacity in the clay is based upon the projected area of an inverted truncated trumpet shape observed in the PIV analyses (see Figure 13 in Teh et al., 2008).

Aside from the fact that the methods of Okamura et al. (1998) and Teh (2007) exhibit inconsistencies that are not logical, i.e. the ϕ'-α relationship in the method of Okamura et al. (1998) and the geometric inconsistency in the method of Teh (2007), the greater problem is that both methods only account for the impact of the initial stress state on the behaviour of the upper sand layer and do not account for the effect of applied stress at failure which is caused by preloading.

2.3 Failure Stress Dependent Method of Lee et al. (2009)

Lee et al. (2009) proposed the failure mechanism in Figure 2, which is based upon the observations of Teh et al. (2008) and the small-strain Finite Element (FE) analyses of Lee (2009). It assumes that an inverted truncated cone of sand with inclination angle equal to the dilation angle (ψ) of the sand is pushed into the underlying clay. Thus q_{peak} is a function of the frictional resistance in the sand, the bearing capacity of the clay and the weight of the sand frustrum.

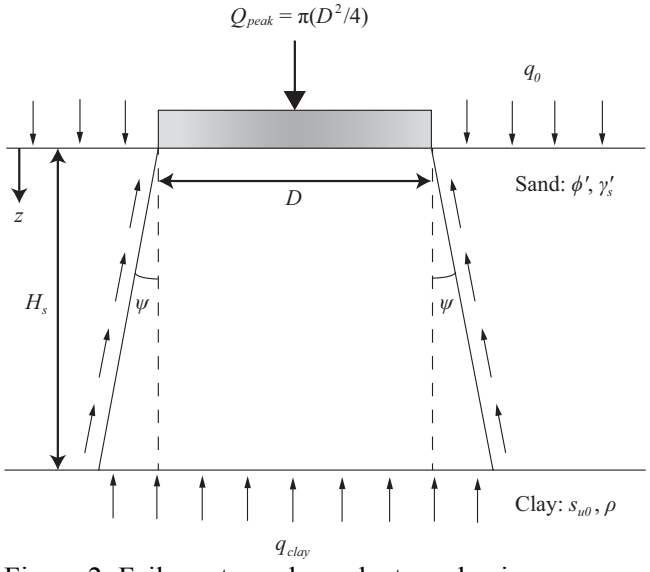

Figure 2: Failure stress dependent mechanism proposed by Lee et al. (2009).

The operative friction angle of the sand layer is related to the peak failure stress (q_{peak}) using a modified version of Bolton's (1986) empirical relationships:

$$I_R = I_D\left(Q - \ln\left(p'\right)\right) - 1 \qquad 0 < I_R < 4 \tag{2}$$

$$\phi' - \phi_{cv} = mI_R \tag{3}$$

$$0.8\psi = \phi' - \phi_{cv} \tag{4}$$

where I_R is a dilatancy indicator, Q is the natural logarithm of the crushing strength of the sand, p' is the mean effective stress and m is a constant related to the stress condition (proposed originally as 5 for plane strain and 3 for triaxial stress). Using a series of FE back-analyses of drum centrifuge tests of foundation penetration on sand overlying clay strata, Lee (2009) proposed a value of 2.65 for m for the scenario where p' is substituted for q_{peak}. Use of these three equations allows both the properties of the sand layer and the angle of inclination of the sand frustrum to be related to the stress level at failure as opposed to the initial in-situ stress state.

Lee (2009) derived a simple design equation for this failure mechanism by treating the sand layer as a series of infinitesimally thin horizontal discs, applying suitable boundary conditions and integrating over the depth of the sand layer, H_s, to yield:

$$\begin{aligned} q_{peak} = {} & \left(N_{c0}s_{u0} + q_0\right)\left(1 + \frac{2H_s}{D}\tan\psi\right)^E \\ & + \frac{\gamma_s' D}{2\tan\psi\left(E+1\right)}\left[1 - \left(1 - \frac{2H_s}{D}E\tan\psi\right)\left(1 + \frac{2H_s}{D}\tan\psi\right)^E\right] \end{aligned} \tag{5}$$

where D is the foundation diameter and the parameter E (used to simplify the algebra) is taken as:

$$E = 2\left[1 + D_F\left(\frac{\tan\phi^*}{\tan\psi} - 1\right)\right] \tag{6}$$

where D_F is an empirical distribution factor relating the local stress at the failure surface to the average vertical stress. It is this parameter D_F that requires calibration. Due to the assumed non-associated behaviour of the sand ($\phi' \neq \psi$) a reduced friction angle, ϕ^*, is used following Drescher and Detournay (1993):

$$\tan\phi^* = \frac{\sin\phi'\cos\psi}{1 - \sin\phi'\sin\psi} \tag{7}$$

For cases where dilation tends to zero, the design equation converges to the following limit:

$$q_{peak} = \left(N_{c0}s_{u0} + q_0\right)e^{E_0} + \gamma_s' H_s\left[e^{E_0}\left(1 - \frac{1}{E_0}\right) + \frac{1}{E_0}\right] \tag{8}$$

where the parameter E_0 is taken as:

$$E_0 = 4D_F\sin\phi_{cv}\frac{H_s}{D} \tag{9}$$

This approach utilises sand properties related to the failure stress state, logical failure mechanism geometry and contains only one empirical factor requiring calibration, the distribution factor D_F. Lee (2009) calibrated this empirical factor for flat foundations using a series of twenty-five centrifuge tests performed in the UWA drum centrifuge on dense sand overlying clay. This was achieved by substituting the experimentally measured q_{peak} into Equation (5) before solving for D_F, yielding the following best-fit linear relationship:

$$D_F = 0.726 - 0.219\frac{H_s}{D}; \quad \frac{H_s}{D} \le 1.12 \tag{10}$$

For the generalised spudcan foundation geometry (the same as used in this investigation which is illustrated in Figure 3) five centrifuge tests on dense sand overlying clay were utilised in a similar calibration, with a combination of the following relationships being proposed to define D_F in relation to H_s/D:

$$D_F = 1.333 - 0.889\frac{H_s}{D}; \quad \frac{H_s}{D} \le 0.9 \tag{11}$$

$$D_F = 0.726 - 0.219\frac{H_s}{D}; \quad 0.9 < \frac{H_s}{D} \le 1.12 \tag{12}$$

The bi-linear nature of this relationship for D_F was attributed to the conical geometry of the model spudcans tested. It was postulated that the conical base of the spudcans caused increases in lateral stress (and consequently average stress at the failure surface in the sand layer) during embedment and some progressive failure (see White et al., 2008) of the sand beneath the spudcan. The increase in lateral stress can be seen to be the dominant phenomena since the D_F for a spudcan foundation is larger than that for a flat footing where $H_s/D < 0.9$. Thus due to the separate calibrations used for the flat footing and spudcan geometries, the distribution factor, D_F, simultaneously accounts for the impact of geometry, increases in lateral stress and progressive failure.

Using Equations (2) to (12) in a simple iterative calculation method (such as a spreadsheet analysis in MS Excel) allows predictions of q_{peak} to be obtained. This method is superior to using design curves or tables since it also allows sensitivity analyses to be conducted rapidly on variables with significant uncertainty (i.e. in-situ measurements of soil strength). Lee (2009) demonstrated the superiority of this failure stress dependent approach over the current best practice recommended by SNAME (2002) and the initial stress dependent methods of Okamura et al. (1998) and Teh (2007). An additional series of nineteen centrifuge model tests sourced from the literature (which was not used to calibrate the model) was used to validate the new approach. The new failure stress dependent model yielded the best prediction of q_{peak} on average, the smallest standard deviation and minimal bias or skew in relation to H_s/D.

2.4 Aim of the Current Investigation

Although Lee (2009) demonstrated the superiority of the new failure stress dependent failure mechanism approach it has a distinct limitation. For spudcans it was calibrated using only five experimental data points and a single height (H_s = 6.2 m) of dense sand (I_D = 92%) overlying clay. It was also only validated using data from three additional tests performed on loose to moderately loose sand overlying clay that had been reported in the literature. To address this limitation a series of fifteen drum centrifuge tests of spudcans penetrating loose sand overlying clay was carried out and combined with the existing five tests of Lee (2009) performed on dense sand overlying clay. This paper summarises the tests and their impact on the calibration and performance of the failure stress dependent model proposed by Lee et al. (2009).

3 EXPERIMENTAL METHOD

3.1 Apparatus

The drum centrifuge at UWA was used to model the penetration of a spudcan into loose sand overlying clay. In brief the drum centrifuge has a 200 mm deep, 300 mm wide continuous channel with radius of 400 mm to the sample surface. It can spin at 200 *g* during testing. The large sample surface area allows detailed parametric experimental investigation to be performed in a single sample with in-situ stress similitude. Thus the stress dependent dilatancy and strength of the sand layer is modelled appropriately.

This investigation utilised a spudcan of the same generalised geometry as the investigation of Lee (2009) and Teh et al. (2007; 2008) and is illustrated in Figure 3. Model spudcans with diameters in the range of 30-100 mm were machined with constant tip and spigot angles as indicated in Figure 3, thus keeping any geometric effects constant between tests of differing scale and geometry. At 200 *g* this gives a prototype diameter range of 6-20 m.

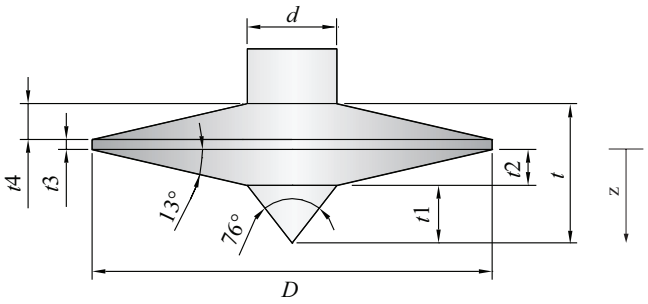

Figure 3: Generalised spudcan geometry used in experimental investigations.

Commercially available Super Fine Silica Sand (SFSS) and kaolin clay identical to those used by Lee (2009) were used in this experimental investigation. The relevant geotechnical properties of these two materials have been investigated extensively at UWA and are reported by Cheong (2002) and Stewart (1992) for the sand and clay respectively.

3.2 Sample Preparation

Kaolin clay was mixed to a water content of 120% and placed in the drum centrifuge channel at 20 *g* until the channel was full, before consolidation to 300 *g*. Following consolidation the sample surface was scraped back using a tool table mounted device to a target clay height of 150 mm. A fabric membrane was then placed on top of the clay and sand was wet pluviated at a rapid rate at 20 *g* onto the fabric membrane, producing a loose sand layer. This was scraped back to a target sand height of 30 mm before the sample was again consolidated to 300 g. The surcharging sand layer and fabric membrane were then removed, before the sand layer was laid again at 20 *g* following the same methodology. This approach ensured that the sand layer on top of the clay was undisturbed prior to testing (settlement of the clay during over-consolidation at 300 *g* caused a rupture in the sand at the split in the fabric membrane). All tests were conducted at 200 g, thus the clay had an OCR of at least 1.5.

3.3 Test Procedure

Assuming a c_v of 2 m^2/year for the clay undrained deformation was ensured by maintaining a dimensionless velocity of 120 for all tests using the following relationship (Randolph and Hope, 2004):

$$V = \frac{vD}{c_v} \tag{13}$$

where v is the penetration velocity and c_v is the coefficient of consolidation. Assuming a c_v of 60,000 m^2/year for sand in Equation (13) yielded $V < 0.01$, indicating drained deformation in the sand.

The assumed c_v values were deemed accurate enough for defining suitable penetration rates. Three sets of tests were performed with the same base clay layer coupled with prototype sand layer heights of 6, 5 and 3.2 m. This was achieved by scraping the sand layer back to a new depth after each set of tests. Five tests were performed on each layer height (with each in a different undisturbed location) yielding fifteen data points in the range of $0.16 \leq H_s/D \leq 1.0$.

3.4 Sample Property Measurement

The relative density of the sand layer was measured using four 60 mm diameter samples, indicating moderately loose sand with average relative density, I_D, of 43%. Correspondingly, the effective unit weight of the sand γ'_s was 10 kN/m^3. The effective unit weight of the clay γ'_c was measured using 20 mm diameter samples extracted using a tube sampler and was found to be 7.11 kN/m^3. Using similar methods Lee (2009) found that for the dense sand tests, I_D of the sand was 92%, γ'_s was 11 kN/m^3 and γ'_c was 7.5 kN/m^3.

T-Bar penetrometer tests were performed on the clay samples following removal of the sand layer (to avoid the impact of entrapped sand beneath the penetrometer following the procedure of Lee (2009)) using a T-Bar factor, $N_{T\text{-}Bar}$ of 10.5 at 200 g. The measured shear strength profile was related to that evident when the sand layer was in-situ using the following relationship:

$$\frac{s_u}{\sigma'_v} = aOCR^b \tag{14}$$

where s_u is the undrained shear strength, σ'_v is the vertical effective stress, OCR is the over consolidation ratio. The parameters a and b were taken as 0.16 and 0.74 in this investigation and 0.185 and 0.84 by Lee (2009), yielding the sand-clay interface shear strength and gradients given in Table 1.

Table 1: Sand-clay interface shear strength and gradients derived from T-Bar testing (* after Lee, 2009).

Test Series	s_u (kPa)	ρ (kPa/m)
H_s = 6.0 m; I_D = 0.43	12.97	1.54
H_s = 5.0 m; I_D = 0.43	12.37	1.54
H_s = 3.2 m; I_D = 0.43	11.02	1.55
H_s = 6.2 m; I_D = 0.92	17.70*	2.0*

4 RESULTS

Figure 4 presents two extreme cases of punch-through with the load measurement reference point as denoted in Figure 3: case (a) with a high H_s/D ratio of 0.78 and dense sand with I_D of 92%, which causes severe punch-through and post-peak softening (data from Lee, 2009) and case (b) with a lower H_s/D ratio and loose sand with I_D of 43%, which causes rapid run-out and no post-peak softening. These two cases demonstrate that punch-through is a risk for both loose and dense sand layers of varying height overlying soft clay and how q_{peak} was identified as the maximum penetration resistance attained in the sand layer.
Following analysis of all penetration tests and identification of q_{peak} in each, the distribution factor D_F was optimized for each test using Equations (2) to (7) by inputting the experimentally measured q_{peak} into Equation (5) and solving iteratively for D_F. These optimal D_F values are presented in Figure 5 (a) versus the original bi-linear relationship governed by Equations (11) and (12), with a coefficient of determination, R^2, of 0.89. Figure 5 (b) presents the same data versus an improved non-linear relationship governed by Equation (15), giving an improved coefficient of determination, R^2, of 0.98.

$$D_F = 0.569\left(\frac{H_s}{D}\right)^{-0.596} \quad ; \quad 0.16 \leq \frac{H_s}{D} \leq 1.0 \tag{15}$$

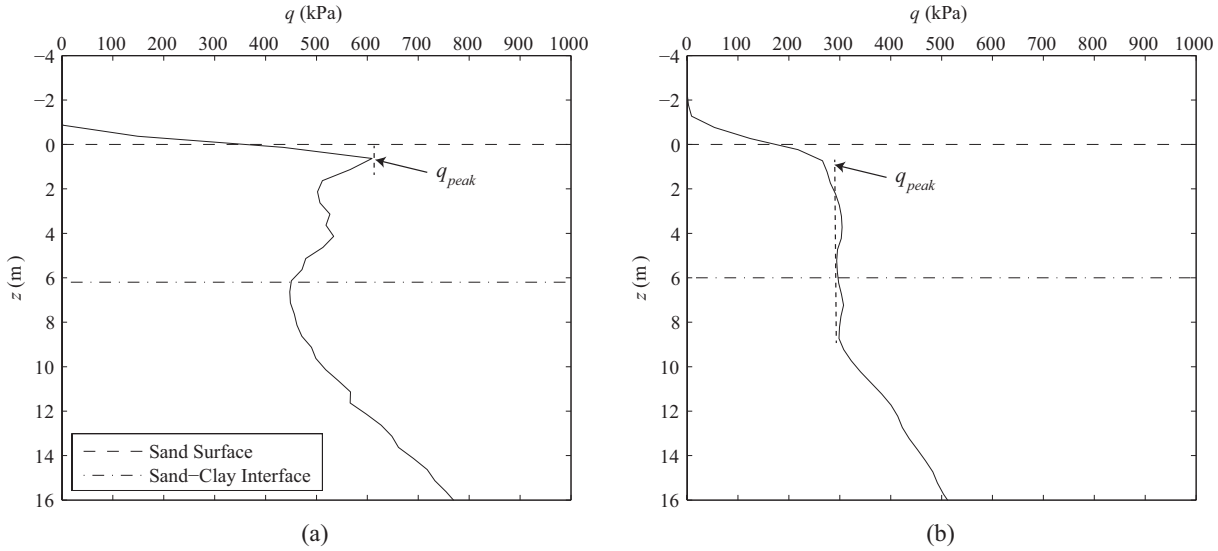

Figure 4: Extreme cases: (a) severe punch-through for thick and dense sand layer after Lee, 2009 (D = 8 m; H_s/D = 0.78; I_D = 92%) and (b) rapid run-out for thin loose sand layer (D = 14 m; H_s/D = 0.43; I_D = 43%).

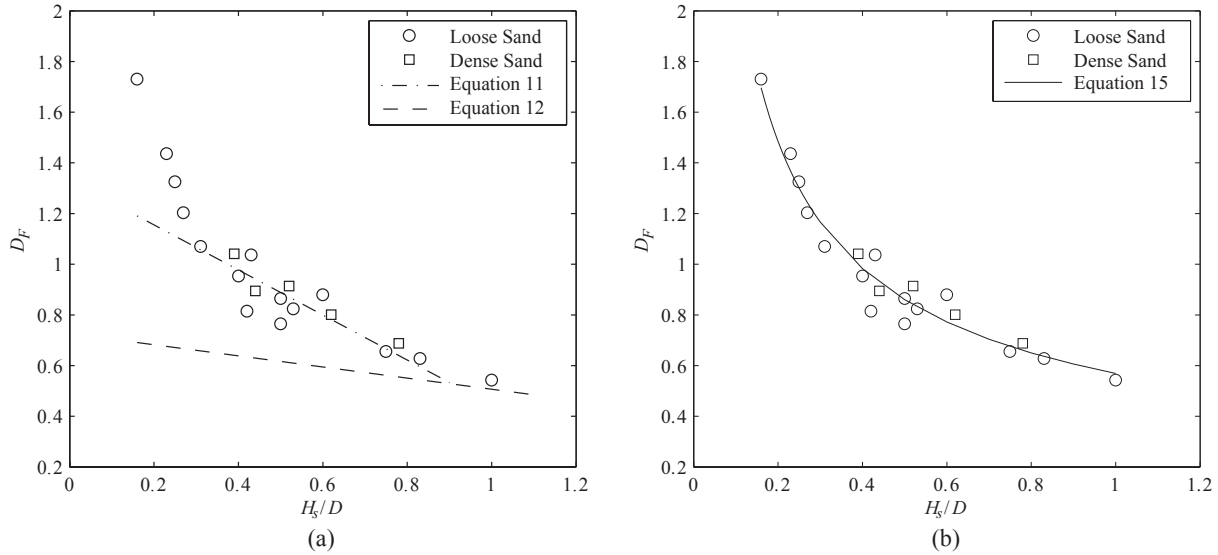

Figure 5: Calibration of distribution factor D_F with respect to H_s/D ratio versus (a) original bi-linear relationships and (b) improved non-linear relationship.

This new non-linear calibration better fits the optimised D_F values, particularly for low H_s/D. It is also more logical since Lee (2009) originally suggested that the two linear lines meet at H_s/D equal to 0.9, due to the diminishing impact of increases in lateral stress due to the embedded geometry of the spudcan at mobilisation of q_{peak}. In reality, embedment of a conical ended spudcan will always cause some increase in lateral stress and thus average stress at the failure surface along the boundary edges of the penetrating sand frustrum. Thus, the fact that Equations (10) and (15) (the D_F calibration lines for a flat footing and the new non-linear relationship proposed for spudcans) do not meet over the range $0.16 \leq H_s/D \leq 1.12$ suggests that the new D_F calibration for spudcans is more logical as well as accurate for a greater range of H_s/D. To assess the impact of the improved D_F calibration, the original bi-linear and new non-linear D_F relationships were substituted into Equations (2) to (7) and solved for q_{peak} iteratively for all twenty penetration tests reported here.

Figure 6 presents the performance of the original bi-linear calibration and Figure 7 presents the performance of the improved non-linear calibration. Figure 6 shows that the original bi-linear relationship causes distinct skew towards under-prediction at low H_s/D and that more than 25% of the tests lie outside the ±10% lines. In contrast Figure 7 indicates that the non-linear relationship adopted significantly mitigates this tendency to skew with H_s/D and all but 15% of the tests lie within the ±10% lines.

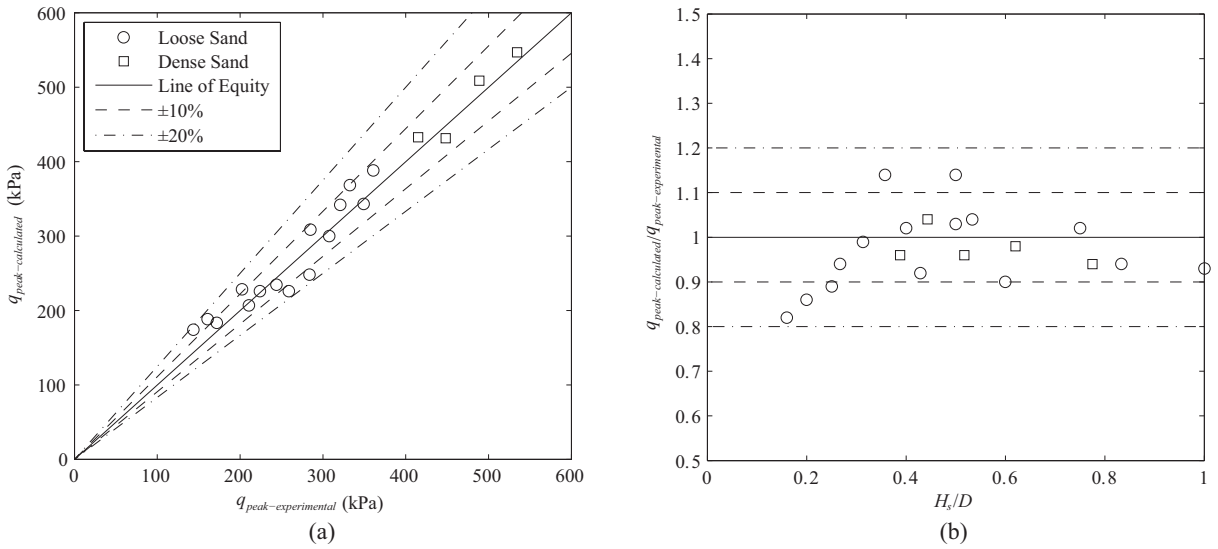

Figure 6: Performance of failure stress dependent model with original bi-linear calibration: (a) $q_{peak\text{-}calculated}$ vs. $q_{peak\text{-}experimental}$ and (b) $q_{peak\text{-}calculated}/q_{peak\text{-}experimental}$ vs. H_s/D.

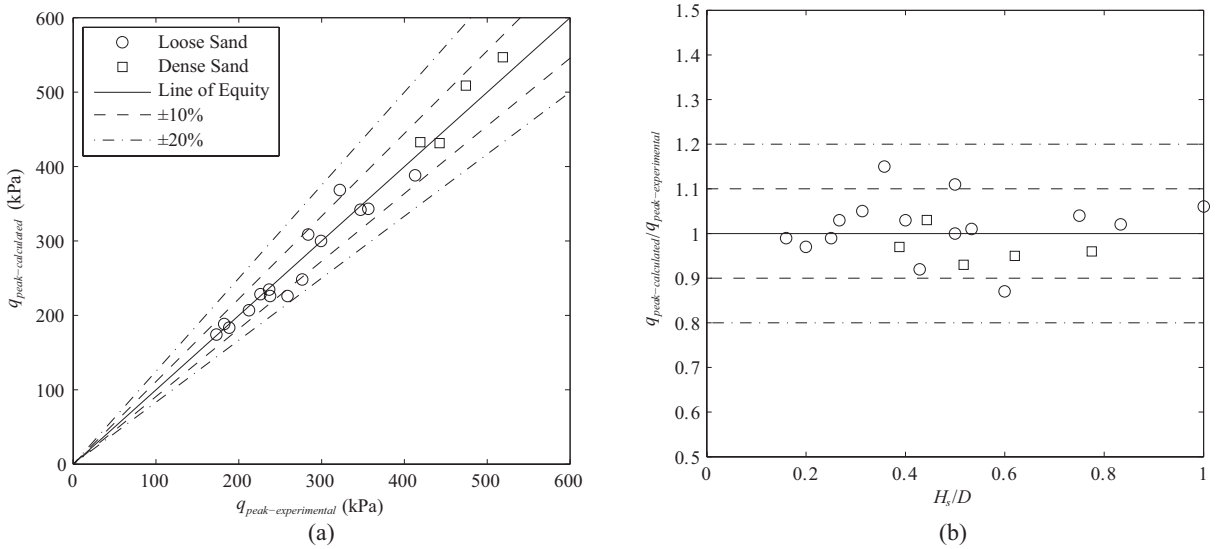

Figure 7: Performance of failure stress dependent model with improved non-linear calibration: (a) $q_{peak\text{-}calculated}$ vs. $q_{peak\text{-}experimental}$ and (b) $q_{peak\text{-}calculated}/q_{peak\text{-}experimental}$ vs. H_s/D.

The results also demonstrate that the failure stress dependent model proposed by Lee et al. (2009) is very capable of dealing with both loose minimally dilatant and dense highly dilatant sands and accurately predicting q_{peak} during punch-through or rapid run-out. The reduction in skew caused by the recalibration performed here also highlights that it was more perhaps important to increase the range of spudcan geometries investigated and incorporated into the calibration rather than the range of relative densities tested. With the improved non-linear calibration for spudcans the failure stress dependent model of Lee et al. (2009) is capable of producing more accurate q_{peak} predictions for a wider range of soil properties and problem geometries.

5 CONCLUSIONS

To reassess the performance and calibration of the failure stress dependent model of Lee et al. (2009) for predicting punch-through on sand overlying clay strata five penetration tests performed by Lee (2009) on dense sand have been combined with an additional set of tests performed in the same manner on loose sand overlying clay. The additional data has demonstrated that the model is very capable of accurately predicting q_{peak}, even in its original form as proposed by Lee et al. (2009). However, following

recalibration the performance has been further improved. The geotechnical centrifuge offered the only realistic method to achieve this recalibration. At present there is no robust constitutive model for sand behaviour that is easily calibrated and accounts for both stress dependent dilatancy and shear-strain softening, hence a numerical approach was not feasible. There is also insufficient data from field studies of punch-through on sand overlying clay strata for the calibration to be performed using back-calculation of past failure events. This investigation demonstrates how the geotechnical centrifuge can be used to calibrate numerical models accurately and economically for a wide range of soil properties and geometries, whilst maintaining scale and stress similitude with the prototype problem.

6 ACKNOWLEDGEMENTS

The work forms part of the activities of the Centre for Offshore Foundation Systems (COFS), which is supported by the State Government of Western Australia and the Lloyd's Register Educational Trust as a Centre of Excellence and now forming one of the primary nodes of the Australian Research Council Centre of Excellence in Geotechnical Science and Engineering. The authors are grateful for this support and also to drum centrifuge technician Mr. Bart Thompson for his assistance during the experimental work and to Dr. Kok Kuen Lee for providing data on the original dense sand over clay experiments.

REFERENCES

Baglioni, V.P., Chow, G.S. and Endley, S.N. (1982). Jack-up rig foundation stability in stratified soil profiles. *Proceedings of Offshore Technology Conference*. Houston. 3-6 May 1982, OTC 4409.

Bolton, M.D. (1986). The strength and dilatancy of sands. *Géotechnique*, **36**(1): 65-78.

Cheong, J. (2002). Physical testing of jack-up footings on sand subjected to torsion. *Honours Thesis*, University of Western Australia.

Drescher, A. and Detournay, E. (1993). Limit load in translational failure mechanisms for associative and non-associative materials. *Géotechnique*, **43**(3): 443-456.

Hanna, A.M., and Meyerhof, G.G. (1980). Design charts for ultimate bearing capacity of foundations on sand overlying soft clay. Canadian Geotechnical Journal, **17**: 300-303.

Lee, K.K., 2009. Investigation of potential punch-through failure on sands overlaying clay soils. *Ph.D. Thesis*, The University of Western Australia.

Lee, K.K., Randolph, M. F. & Cassidy, M. J. (2009). New simplified conceptual model for spudcan foundations on sand overlying clay soils. Offshore Technology Conference, OTC20012.

Okamura, M., Takemura, J. and Kimura, T. (1998). Bearing capacity predictions of sand overlying clay based on limit equilibrium methods. Soils and Foundations, **38**(1):181-194.

Osborne, J.J. and Paisley, J.M. (2002). E Asia jack-up punch-throughs: The way forward? *Proceedings of the International Conference on Offshore Site Investigation and Geotechnics - Sustainability and Diversity*. London. November 2002. pp. 301-306.

Randolph, M.F. and Hope, S. (2004). Effect of cone velocity on cone resistance and excess pore pressures. Proceeding of International Symposium on Engineering Practice and Performance of Soft Deposits. Osaka, Japan. pp. 147-152.

SNAME (2002). Guidelines for site specific assessment of mobile jack-up units, Society of Naval Architects and Marine Engineers, Technical and Research Bulletin 5-5A, New Jersey.

Stewart, D.P. (1992). Lateral loading of piled bridge abutments due to embankment construction. *Ph.D. Thesis*, The University of Western Australia.

Teh, K.L. (2007). Punch-through of spudcan foundation in sand overlying clay. *PhD Thesis*, National University of Singapore.

Teh, K.L., Cassidy, M.J., Leung, C.F., Chow, Y.K., Randolph, M.F. and Quah, M. (2008). Revealing the bearing capacity mechanisms of a penetrating spudcan through sand overlying clay. *Géotechnique*, **58**(10): 793-804.

White, D.J., Teh, K.L., Leung, C.F. and Chow, Y.K. (2008). A comparison of the bearing capacity of flat and conical circular foundations on sand. *Géotechnique*, **58**(10): 781-792.